

# Data-Driven Control of Highly Interactive Systems using 3DoF Model-On-Demand MPC: Application to a MIMO CSTR \*

Sarasij Banerjee \* Owais Khan \* Mohamed El Mistiri \*  
Naresh N. Nandola \*\* Daniel E. Rivera \*

\* Control Systems Engineering Laboratory, School for Engineering of  
Matter, Transport, and Energy, Arizona State University, Tempe, AZ  
85287 USA

\*\* Siemens Technology, Princeton, NJ 08540 USA

**Abstract:** This paper presents a Three-Degree-of-Freedom Model Predictive Control (3DoF MPC) framework based on Multi-Input-Multi-Output (MIMO) “Model-on-Demand” (MoD) estimation. MoD is a data-centric weighted regression algorithm that generates local models over adaptively varying neighborhoods of changing operating conditions. The 3DoF formulation enables individualized tuning of parameters relating to setpoint tracking and measured and unmeasured disturbance rejection. Online estimation of system dynamics using MIMO MoD and augmentation with the 3DoF MPC structure allows the generation of control laws based on efficient locally linear approximations of system nonlinearities. This paper evaluates the framework through a case study involving a nonlinear MIMO Continuous Stirred Tank Reactor (CSTR) model. The MIMO CSTR system is highly interactive, making data-driven estimation and control notably more challenging than its SISO counterpart. The generation of an informative database using modified “zippered” multisines is presented. The paper concludes with a case study demonstrating the effectiveness of 3DoF MoD MPC in achieving constrained MIMO control of reactor concentration and temperature in the presence of disturbances through a flexible and intuitive approach.

**Keywords:** data-based control, nonlinear system identification, time-varying systems, model predictive control, process control

## 1. INTRODUCTION

Data-driven methodologies have significantly expanded the class of complex systems being studied in the context of system identification and control. These have gained attention due to their ability to address modeling and control complexities of nonlinear systems in the absence of efficient *a priori* models (Carnerero et al., 2023; Piga et al., 2018). Nonlinear MIMO systems, in particular, present a class of problems that are inherently difficult to control due to the combined challenges of nonlinearities and interactions (Häggblom and Böling, 1998; Rivera et al., 2007). While many data-centric estimation and control algorithms implemented in MIMO settings satisfy predictive requirements, they may suffer from reduced interpretability and high architectural complexity. Therefore, integrated modeling and control approaches meeting fundamental and practical needs are essential for such systems. This paper presents a multivariable “Model-on-Demand”-based multi-degree-of-freedom MPC framework to address these challenges.

“Model-on-Demand” (MoD) estimation has been widely studied in the literature in the context of open-loop estimation and closed-loop model-based control (Stenman,

\* Support for this research has been provided by NIH grants R01LM013107 and R01CA244777 and NSF grant CBET 2200161.

1999; Braun, 2001; Nandola and Rivera, 2010). MoD can be conceptualized as a composite of global and local modeling that uses an informative database to represent best the changing operating conditions at each time instant, thereby generating appropriate models “on demand”. This provides the sophistication of global nonlinear estimation algorithms while preserving the simplicity of linear and local estimation approaches. The 3DoF MPC algorithm provides an improved formulation that allows independent regulation of parameters related to setpoint tracking, measured disturbance rejection, and unmeasured disturbance rejection (Nandola and Rivera, 2013; Khan et al., 2022). When augmented with the MoD-based predictive models estimated online, the 3DoF MPC provides an efficient and robust nonlinear control architecture in the SISO setting (Nandola and Rivera, 2010). However, the MIMO case presents additional complexities regarding system identification and control. This paper aims to extend the existing literature by formulating a MIMO MoD estimation framework and implementing it in a closed-loop setting using the 3DoF MPC structure through an intuitionistic state-space approach. The concept is validated through a case study involving a highly interactive MIMO variant of the well-known Continuous Stirred Tank Reactor (CSTR) model (Bequette, 2003). It is demonstrated that MoD, through judicious data selection, adapts well to nonlinearity and

directionality. It exhibits superior control over the conventional ARX-based MPC architecture in a 3DoF setting.

The paper is organized as follows: Section 2 covers the MoD estimation and the corresponding 3DoF MPC formulation. Section 3 describes the reactor dynamics and an input signal design for informative data collection, the MoD-based open-loop estimation, and a comparative study involving the ARX estimation. It finally discusses the culminating closed-loop control achieved using the 3DoF MoD MPC framework and demonstrates its advantage over the ARX-based controller. Section 4 concludes the paper with directions for future work.

## 2. MOD-BASED NONLINEAR IDENTIFICATION AND MIMO CONTROL

This section describes the kernel-based weighted regression involved in MoD estimation and its connection to the 3DoF MPC framework. The identification problem can be formulated at each time instant based on system measurements to generate models that minimize simulation error. Such models can be generated in open and closed-loop settings to estimate the desired dynamics effectively.

### 2.1 Formulation of the identification problem

MoD identification problem (Stenman, 1999) can be described as follows: assume a system dynamic can be modeled as  $y_c = m(\varphi_c) + e_c$  at a current operating point  $c$ , where  $\varphi_c = [y_{c-1} \dots y_{c-n_a} \bar{u}_{c-n_b} \dots \bar{u}_{c-n_b-n_k+1}]^T$  is the regressor at the current operating point (collection of past system inputs and outputs in either open-loop or closed-loop settings) based on an ARX regressor structure  $[n_a \ n_b \ n_k]$ . Given a noisy dataset of input-output measurements  $(X_k, Y_k)_{k=1}^N$ , fit a local polynomial (preferably linear or quadratic)  $\hat{m}(\varphi_k, \theta_c)$  over an adaptively varying neighborhood of the current operating point based on a local Taylor Series expansion by evaluating the least-squares solution of the parameter estimation problem:

$$\hat{\theta}_c = \arg \min_{\theta_c} \sum_{k=1}^N \ell(y_k - \hat{m}(\varphi_k, \theta_c)) K_h \left( \frac{\|\varphi_k - \varphi_c\|_M}{h} \right) \quad (1)$$

$\ell(\cdot)$  is a scalar-valued positive norm function (usually the 2-norm).  $\hat{\theta}_c = [\hat{\theta}_0 \ \hat{\theta}_1]$  represents the set of parameters of the design matrix  $[1 \ \tilde{\varphi}^T \dots (\tilde{\varphi}^p)^T]$  arising from the polynomial modeling of the regressors, where  $\tilde{\varphi} = \varphi_k - \varphi_c$  is the distance between the current regressor and the  $k^{th}$  regressor in the dataset,  $p$  is the polynomial degree, and  $\hat{\theta}_1 \in \mathbb{R}^{p_{reg}}$  is the vector of the polynomial coefficients. The length  $p_{reg}$  of the parameter vector is determined by the length  $d_{reg}$  of the regressor vector.  $p_{reg} = d_{reg}$  for the linear case, and  $p_{reg} = d_{reg} + d_{reg}(d_{reg} + 1)/2$  for the quadratic case.  $K_h(\cdot)$  is a kernel-based weight function whose bandwidth parameter is given by  $h$ . Weights are given to the neighboring points based on a scaled distance function  $\|\tilde{\varphi}\|_M = \sqrt{\tilde{\varphi}^T M \tilde{\varphi}}$ , where  $M$  is the inverse of the covariance matrix of the regressors. The adaptive bandwidth is implemented in practice through an iterative procedure involving a user-defined range  $[k_{min}, k_{max}]$  for neighborhood size.

### 2.2 Evaluation of the MoD-based predictive model

MIMO identification typically involves the estimation of each output as a Multi-Input-Single-Output (MISO) model of the system inputs as well as of other outputs, followed by organizing these models to form an augmented MIMO estimator. For the  $i^{th}$  output  $y_i$ , assuming  $\hat{m}_i(\varphi_k, \hat{\theta}) = \hat{\theta}_{i,0} + \hat{\theta}_{i,1}^T (\varphi_k - \varphi_c)$  to be a locally linear model, and  $\hat{\theta}_{i,0}$  and  $\hat{\theta}_{i,1}$  to be the optimal parameter values, a one-step ahead estimate for  $y_i$  can be calculated as follows:

$$\hat{y}_{i,k} = \alpha_i + \hat{\theta}_{i,1}^T \varphi_k \quad (2)$$

where  $\alpha_i = \hat{\theta}_{i,0} - \hat{\theta}_{i,1}^T \varphi_c$ . The time series model thus generated from the MoD-based estimation can be generalized for the MIMO setting to evaluate state-space matrices needed for defining a piecewise affine (PWA) predictive structure of the form:

$$x_{k+1} = Ax_k + B\bar{u}_k + f \quad (3)$$

$$y_k = Cx_k + d'_k \quad (4)$$

where  $x_k \in \mathbb{R}^{n_x}$  and  $\bar{u}_k \in \mathbb{R}^{n_u+n_{dist}}$  represent the states and the inputs of the system respectively.  $\bar{u}_k$  can be separated into  $n_u$  manipulated variables ( $u_k \in \mathbb{R}^{n_u}$ ) and  $n_{dist}$  disturbances ( $d_k \in \mathbb{R}^{n_{dist}}$ ).  $y_k \in \mathbb{R}^{n_y}$  represents the measurable process output vector, and  $d'_k$  is the lumped representation of unmeasured disturbances and noises in the outputs. The  $A$ ,  $B$ , and  $C$  matrices are determined from  $\theta_1$ , and the scalar  $f$  is generated from  $\alpha$  at each time step. The  $B$  matrix can be split into  $B_u$  and  $B_d$ , corresponding to  $u_k$  and  $d_k$ , respectively. Furthermore,  $d'_k$  is considered to be a stochastic signal and can be described through a state-space representation:

$$\zeta_{k+1} = A_w \zeta_k + B_w w_k \quad (5)$$

$$d'_k = C_w \zeta_k \quad (6)$$

where  $w_k$  is an integrated white noise. It is assumed that the disturbance vector  $d'_k$  consists of uncorrelated components.  $B_w = C_w = I$  and  $A_w = \text{diag}\{\Lambda_1, \dots, \Lambda_{n_y}\}$  where the entries of matrix  $A_w$  have values of 0 for single-integrating disturbances and 1 for double-integrating disturbances. This structure allows us to formulate an extended state-space model (Nandola and Rivera, 2013):

$$X_{k+1} = AX_k + \mathcal{B}_u \Delta u_k + \mathcal{B}_d \Delta d_k + \mathcal{B}_w \Delta w_k \quad (7)$$

$$y_k = CX_k \quad (8)$$

for zero offsets to integrating unmeasured disturbances.

### 2.3 MoD-based controller formulation

MIMO MoD can be implemented in a closed-loop setting to perform online estimation through locally linearized approximations of system dynamics based on system measurements at each time instant and the open-loop training dataset. The salient features of the 3DoF MoD MPC architecture include a database storing the open-loop estimation data, a local polynomial generator, and a MoD-based optimizer, as illustrated in Fig.1. As the operating conditions change, the MoD algorithm generates predictive models in closed-loop that evolve using "most relevant" data at each time instant. This is achieved by placing the current operating point in the regressor space of the dataset characterized by the  $[n_a \ n_b \ n_k]$  structure used to create the open-loop dataset and drawing a suitable

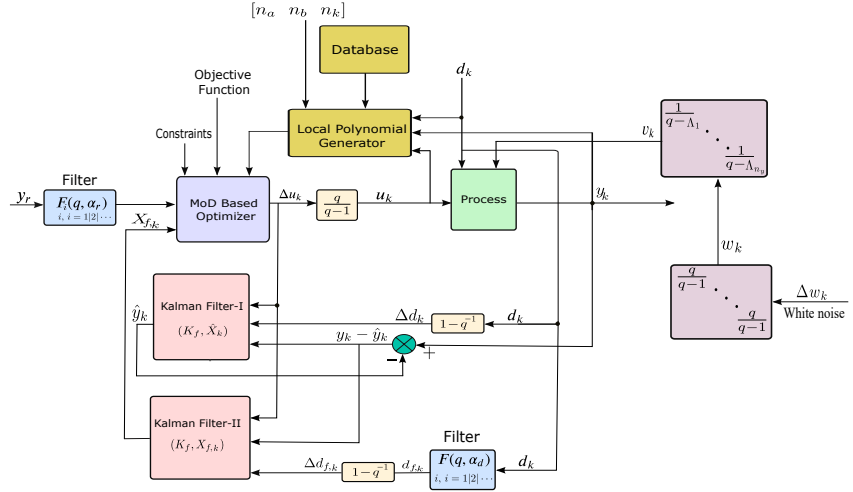


Fig. 1. MoD-Based MPC for setpoint tracking of a process subject to constraints, measured and unmeasured disturbances. Kalman Filter-I refers to (17)-(18) and Kalman Filter-II refers to (20)-(21)

neighborhood of data points that best represent that operating point, followed by local polynomial modeling of this neighborhood. The local polynomial is then rearranged to evaluate the time-varying state-space matrices for the predictive model as demonstrated in (3)-(4). These matrices form the basis of the control law evaluated by the optimizer at each time step by minimizing:

$$\min_{u_{k+i}} \sum_{i=1}^p \| (y_{k+i} - y_{r,k+i}) \|_{W_y}^2 + \sum_{i=0}^{m-1} \| (\Delta u_{k+i}) \|_{W_{du}}^2 \quad (9)$$

$$\text{s.t. } y_{\min} \leq y_{k+j} \leq y_{\max}, \quad 1 \leq j \leq p \quad (10)$$

$$u_{\min} \leq u_{k+i} \leq u_{\max}, \quad 0 \leq i \leq m-1 \quad (11)$$

$$\Delta u_{\min} \leq \Delta u_{k+i} \leq \Delta u_{\max}, \quad 0 \leq i \leq m-1 \quad (12)$$

where  $p$  is the prediction horizon,  $m$  is the control horizon,  $\|(\cdot)\|_{W_*} \triangleq \sqrt{(\cdot)^T W_* (\cdot)}$  is the vector 2-norm weighted by matrix  $W_* > 0$  for the respective process variable, and  $(\cdot)_r$  is the corresponding reference trajectory.

The 3DoF formulation (Nandola and Rivera, 2013; Khan et al., 2022) refers to the independent regulation of parameters related to setpoint tracking ( $\alpha_r$ ), measured disturbance rejection ( $\alpha_d$ ), and unmeasured disturbance rejection ( $f_a$ ) based on their desired closed-loop time constants, where  $\alpha_r = e^{T_s/\tau_r}$ ,  $\alpha_d = e^{T_s/\tau_d}$ , and  $f_a = (1 - e^{T_s/\tau_u})$ .  $T_s$  denotes the sampling time.

*Setpoint and Measured Disturbance Filtering* To generate filtered output reference trajectory  $y_r$ , the following transfer function is used:

$$\frac{y_{r,k+i}}{y_{\text{target}}} = f(q, \alpha_r^j), \quad 1 \leq j \leq n_y, \quad 1 \leq i \leq p \quad (13)$$

where  $f(q, \alpha_r^j)$  is a Type-I filter for the  $j$ -th reference:

$$f(q, \alpha_r^j) = \frac{(1 - \alpha_r^j)q}{q - \alpha_r^j}, \quad 0 \leq \alpha_r^j < 1, \quad 1 \leq j \leq n_y \quad (14)$$

$\alpha_r^j$  is the tuning parameter to adjust the desired speed of response of each output  $j$  to setpoint change, where a low value for  $\alpha_r^j$  yields a fast output setpoint tracking response. A similar filter is implemented for the measured disturbances. The filter transfer function  $f(q, \alpha_d^j)$  depends on whether the disturbance is asymptotically step or

ramp (*i.e.*, Type-I or Type-II signal). In this paper, we implement Type-I filters for filtering step disturbance signals. It is given by:

$$\frac{d_{f,k+i}}{d_{k+i}} = f(q, \alpha_d^j), \quad 1 \leq j \leq n_{dist}, \quad 0 \leq i \leq p-1 \quad (15)$$

$$f(q, \alpha_d^j) = \frac{(1 - \alpha_d^j)q}{q - \alpha_d^j}, \quad 0 \leq \alpha_d^j < 1 \quad (16)$$

*Measured and Unmeasured Disturbance Rejection using Kalman Filters* State estimation for (7)-(8) is performed through a Kalman Filter approach to achieve multiple degrees of freedom. This involves a two-step process for decoupling the effects of the measured and the unmeasured disturbances. In the first step, an estimate  $\hat{X}_k$  of the state  $X_k$  is generated at each sampling instant by utilizing unfiltered measured disturbances and unmeasured disturbances, as follows:

$$\hat{X}_{k|k-1} = \mathcal{A}\hat{X}_{k-1|k-1} + \mathcal{B}_u \Delta u_{k-1} + \mathcal{B}_d \Delta d_{k-1} \quad (17)$$

$$\hat{X}_{k|k} = \hat{X}_{k|k-1} + \mathcal{K}_f (y_k - \mathcal{C}\hat{X}_{k|k-1}) \quad (18)$$

where  $\mathcal{K}_f$  is the gain matrix, defined as follows:

$$\mathcal{K}_f = [0 \ F_y^T \ F_w^T]^T \quad (19)$$

where

$$F_w = \text{diag} \{ f_w^1, \dots, f_w^{n_y} \} \quad F_y = \text{diag} \{ f_y^1, \dots, f_y^{n_y} \}$$

$$f_y^j = \frac{(f_w^j)^2}{1 + \Lambda_j - \Lambda_j f_w^j}, \quad 1 \leq j \leq n_y$$

$f_w^j \in [0, 1]$  is a user-defined tuning parameter to adjust the speed of response of unmeasured disturbance rejection for each output  $j$  through  $\mathcal{K}_f$ . The terms in the RHS of (17) consider the manipulated variable and the unfiltered measured disturbance input to the system. Consequently, the correction term  $(y_k - \mathcal{C}\hat{X}_{k|k-1})$  in the equation (18) accounts for the unmeasured disturbance in the system; Next, the filtered measured disturbance signal  $d_f$  is utilized along with the unmeasured disturbance to generate a filtered augmented state equation, which in turn is used to generate an estimate of the output, as follows:

$$X_{f,k|k-1} = \mathcal{A}X_{f,k-1|k-1} + \mathcal{B}_u\Delta u_{k-1} + \mathcal{B}_d\Delta d_{f,k-1} \quad (20)$$

$$X_{f,k|k} = X_{f,k|k-1} + \mathcal{K}_f(y_k - \mathcal{C}\hat{X}_{k|k-1}) \quad (21)$$

In this approach, tuning for measured disturbance rejection ( $\alpha_d^j$ ) and tuning for unmeasured disturbance rejection ( $\mathcal{K}_f$ ) remain independent of each other.

### 3. THE CSTR MODEL: A MIMO CASE STUDY

A MIMO model of the highly interactive nonlinear CSTR system is chosen to be a suitable test case for demonstrating the efficacy of the MoD-based 3DoF MPC algorithm. The widely used CSTR model comprises a single exothermic reaction with first-order kinetics taking place in a perfectly mixed non-adiabatic reactor vessel and can be characterized by the following set of differential equations:

$$\frac{dC_A(t)}{dt} = \frac{F(t)}{V}(C_{A_f}(t) - C_A(t)) - r_A(t) \quad (22)$$

$$\begin{aligned} \frac{dT(t)}{dt} = & \frac{F(t)}{V}(T_f - T(t)) - \left(\frac{\Delta H}{C_p \rho}\right) r_A(t) \\ & - \frac{UA}{C_p \rho V}(T_j(t) - T(t)) \end{aligned} \quad (23)$$

$$r_A(t) = k_o \exp\left(\frac{\Delta E}{RT(t)}\right) C_A(t) \quad (24)$$

The system involves manipulating jacket temperature  $T_j(t)$  and feed flow rate  $F(t)$  to control reagent concentration ( $C_A(t)$ ) in the tank and reactor temperature  $T(t)$ . Feed concentration  $C_{A_f}(t)$  is assumed to be constant at  $\bar{T}_f$ , and jacket temperature changes  $\Delta T_j(t)$  are considered disturbances. Other constants include feed temperature  $T_f$ , density ( $\rho$ ), and reacting liquid volume  $V$ . The system exhibits nonlinearities associated with ignition, extinction, and limit cycles (Bequette, 2003). Independent control of concentration and temperature is challenging due to strong interactions between the two. System parameters (Bequette, 2003) are summarized in Table 1.

#### 3.1 Input Signal Design

The desired outcome of MIMO control of the reactor involves increasing the yield (lowering  $C_A$ ) while holding reactor temperature ( $T$ ) constant (the low-gain direction). This, however, is opposite to the high-gain direction of the system where a decrease in  $C_A$  increases  $T$  (due to the exothermic reaction), making it hard to sufficiently excite the desired dynamics for data-driven estimation. This challenge is overcome by designing modified "zippered" multisine input signals based on directionality information

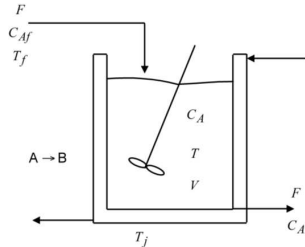


Fig. 2. CSTR model for an exothermic, irreversible reaction.

Table 1. Plant parameters for the CSTR model

Parameter	Value	Parameter	Value
$\Delta H$ (kcal/kgmol)	-5960	$\Delta E$ (kcal/kgmol)	11843
$\rho C_p$ (kcal/m <sup>3</sup> °C)	500	$T_f$ (K)	298.15
$\bar{C}_{A_f}$ (kgmol/m <sup>3</sup> )	10	$UA$ (kcal/m <sup>3</sup> °C hr)	150
$T_j$ (K)	298.15	$C_A$ (kgmol/m <sup>3</sup> )	8.5695
$\bar{T}$ (K)	311.267	$R$ (kcal/kgmol °C)	1.98589

(Rivera et al., 2007). The modified zippered approach excites correlated and uncorrelated harmonics based on user-specified parameters, thereby suitably highlighting both low and high-gain directions. Directionality information can be obtained by considering the steady-state gain matrix  $G_0$  of the linearized first-principle-based model. For the reactor model,  $G_0 = \begin{bmatrix} -0.0565 & 3.2373 \\ 0.7490 & -26.6572 \end{bmatrix}$ .

An SVD analysis reveals that the low-gain direction, corresponding to the smaller singular value  $\sigma_2 = 0.0342$ , points along  $\underline{\nu} = [-0.9996 \quad -0.0279]^T$  in the input regressor space and resultantly along  $G_0\underline{\nu} = [-0.0339 \quad -0.0041]^T$  in the output regressor space.  $\frac{|\underline{\nu}(1)|}{|\underline{\nu}(2)|} = \frac{|-0.9996|}{|-0.0279|} = 35.79$  gives a suitable ratio of amplitudes for the modified zippered input signals for adequately exciting the low-gain direction. The input signals corresponding to the manipulated variable  $T_j$  and  $F$  were generated using the minimum crest-factor algorithm per Guillaume et al. (1991) with modified zippered spectra and sampling time of  $T = 1$  hour, with amplitudes chosen to be 25 K and  $\frac{25}{35.79} m^3/hr = 0.6985 m^3/hr$ , respectively. Furthermore, band-limited white noise with some auto-regressive character was used to generate data corresponding to the measured disturbance. The signal power was chosen to be 1 unit, and the autoregressive filter was  $\frac{0.05}{z(z-0.9)}$ . The signal parameters are summarized in Table 2, and the power spectrum for the modified zippered design is illustrated in Fig. 3. The estimation and the validation signals were generated using different realizations of the input signals with the same frequency content and same amplitude,

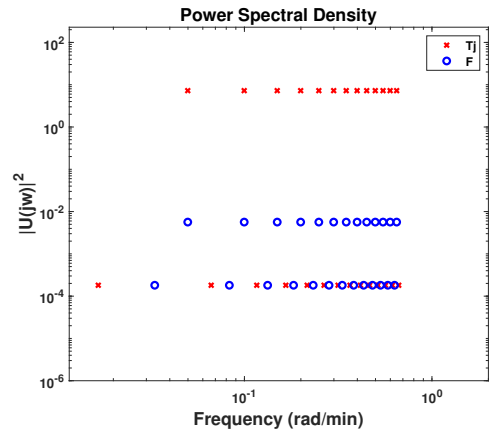


Fig. 3. Plot illustrating the power spectrum corresponding to the modified zippered signals for  $T_j$  and  $F$ .

Table 2. Signal parameters for the design of modified zippered signals.

Parameter	Value	Parameter	Value
$\alpha_s$	2	$\beta_s$	3
$\tau_{dom}^L$	5 hours	$\tau_{dom}^H$	10 hours
high-freq ratio	0	low-freq interval	0
$n_s$	20	$\gamma$	200

and the corresponding outputs were generated by passing these signals through the plant model. Fig. 4 shows the estimation dataset for illustrative purposes.

### 3.2 Open-loop Model-on-Demand Estimation

After an informative dataset is generated, it is standardized to ensure a well-conditioned estimation of the system. For estimation purposes, a locally linear polynomial with a regressor structure of  $[n_a \ n_b \ n_k] = [2 \ 2 \ 1]$  was deemed suitable for parsimoniously describing the data. During estimation, the localized Akaike Information Criterion (AIC) was chosen as a reasonable measure for goodness-of-fit, with a variance penalty of 3. The range  $[k_{min}, k_{max}]$  for neighborhood size was chosen to be  $[45, 100]$  based on the length of the database, and a tricube kernel was selected to weigh the points in the neighborhood. Fig 5 demonstrates a comparison between the open-loop estimation results over the validation dataset for MoD and ARX-based estimators with the same set of parameters in the simulated setting. The goodness of fit measure is evaluated by calculating the normalized root mean square error (NRMSE) fits. As noted in Table 3, MoD-based estimation (fit percentages: 81.28% for  $C_A$  and 53.39% for  $T$ ) demonstrates superior performance over its ARX-based counterpart (fit percentage: 59.03% for  $C_A$  and 27.89% for  $T$ ) in capturing the nonlinearities in the data with significantly higher fit.

### 3.3 Three Degree-of-Freedom MoD MPC

The true effectiveness of the MIMO MoD-based predictive model is realized when it is tested in the closed-loop setting for the simultaneous control of two reactor outputs. Although the 3DoF MPC framework provides a sophisticated and robust control architecture in itself, its performance greatly relies on the choice of the predictive model. A

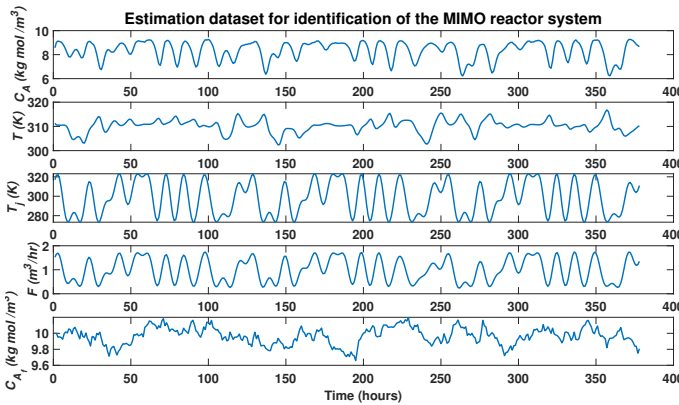


Fig. 4. Estimation datasets for the MIMO CSTR model.

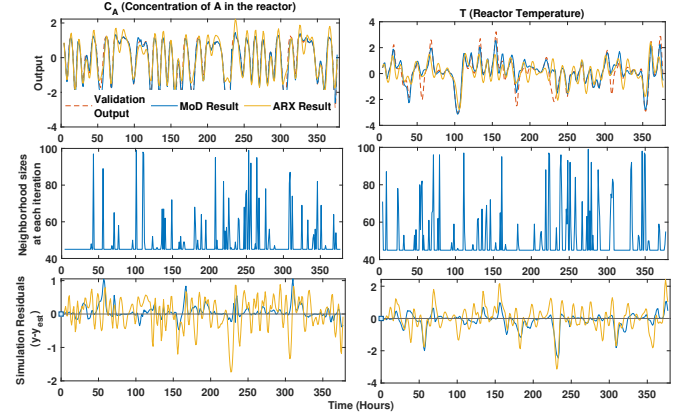


Fig. 5. Comparison of the open-loop MoD and ARX-based simulators on the validation dataset.

comparative case study with a conventional ARX-based predictive model in 3DoF settings under the same set of plant parameters and constraints (summarized in Table 4) demonstrates the ability of the MoD MPC to address loop interactions and nonlinearities of the CSTR model in a superior manner. As shown in Fig 6, a series of set-point changes are introduced in  $C_A$  while the temperature setpoint is held constant at its steady-state value. During its course of operation, the reactor is subjected to a step change  $D_m = \Delta C_{A_f} = 0.2 \text{ kg mol/m}^3$  at time  $t = 160$  hours (measured), and a step change  $D_u = \Delta T_j = 2 \text{ K}$  at  $t = 200$  hours (unmeasured). The MoD-based controller achieves smooth tracking of changes in reference trajectory of  $C_A$  with minimal oscillations and zero offsets, unlike the ARX-based controller, which demonstrates oscillations of large magnitudes that take comparatively longer to settle. Besides the faster setpoint tracking of  $C_A$ , the former controller keeps the deviations in reactor temperature  $T$  from its steady-state value within an acceptable range of 4 K. The ARX-based controller, on the contrary, shows noticeably higher deviations in  $T$  (maximum deviation = 11 K at  $t = 110$  hrs) while trying to achieve setpoint tracking for  $C_A$ , thus making it unsuitable for the control of the reactor system. Fig. 6 clearly illustrates the interactive nature of

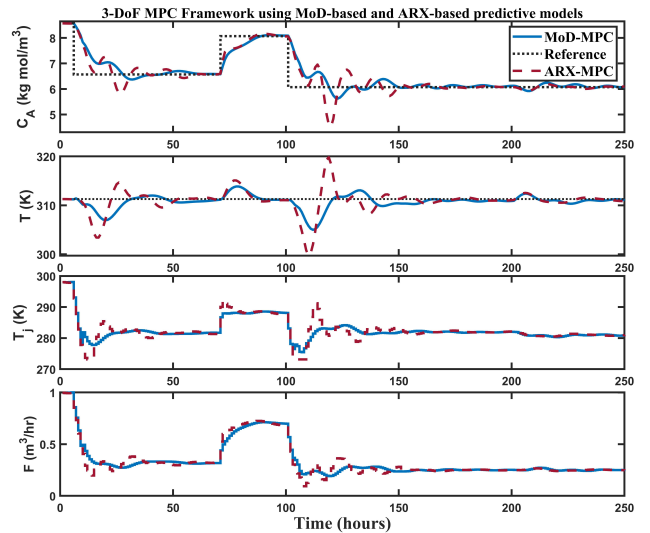


Fig. 6. Closed-loop performance of 3DoF MoD MPC (solid) and 3DoF ARX MPC (dashed).

Table 3. Open-loop Estimation results for MoD vs ARX-based estimators for  $C_A$  and  $T$

Method	$C_A$			$T$		
	NRMSE Fit (%)	RMS Error	Max Error	NRMSE Fit (%)	RMS Error	Max Error
MoD	81.28	0.20	1.05	53.39	0.49	2.45
ARX	59.03	0.45	1.73	27.89	0.76	3.14

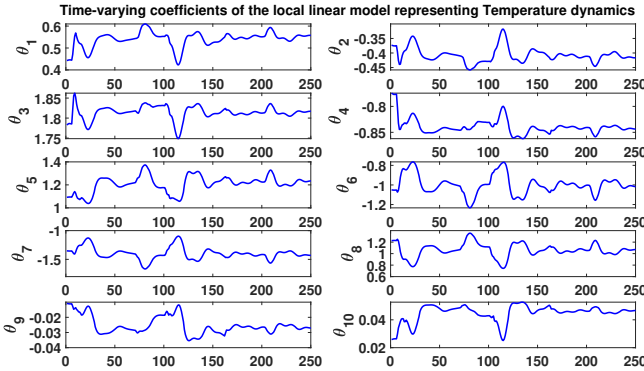


Fig. 7. Time-varying coefficients of the locally linear model for  $T$  based on MoD estimation.  $\theta_1 - \theta_2$  are related to the time-lagged terms for  $C_A$ ,  $\theta_3 - \theta_4$  for  $T$ ,  $\theta_5 - \theta_6$ ,  $\theta_7 - \theta_8$ ,  $\theta_9 - \theta_{10}$  for  $T_j$ ,  $F$ , and  $C_{Af}$  respectively.

the system, which forces the inputs to move in similar directions, making independent control of two outputs a challenging task. The ARX-based controller displays higher sensitivity to the interactive nature of the problem, thereby exhibiting prominent oscillations in manipulated variable response, and it pushes the system to more extreme limits to achieve the performance otherwise easily obtained by the MoD-MPC with notably more feasible manipulated variable responses. The controller based on the MoD estimator generates predictions based on superior linearization of the data in a local neighborhood of each operating point when compared to the controller using the ARX-based globally linear predictive model. Fig. 7 demonstrates the scaled time-varying coefficients of the locally linear dynamic model for *Temperature*. This illustration provides a clear interpretation of the nonlinearities in the system and the corresponding adaptations of the MoD model. This establishes the 3DoF MoD MPC as a better control framework for the highly interactive and nonlinear MIMO CSTR model than the ARX-based 3DoF MPC.

#### 4. SUMMARY AND CONCLUSIONS

The critical component of any model-based control scheme is traditionally a linear predictive model that generates sub-optimal control sequences for highly interactive and nonlinear operating ranges. MoD provides an attractive alternative with superior estimation abilities while preserving the accessibility of linear techniques. However, the

Table 4. Control design parameters for the MIMO CSTR problem

Par	Value	Par	Value
$p$	50	$y_{min}$	$[-\infty -\infty]$
$m$	20	$y_{max}$	$[\infty \infty]$
$\tau_r$	[10 10] hrs	$\Delta u_{min}$	$[-5 \text{ K} -0.2 \text{ m}^3/\text{h}]$
$\tau_d$	5 hrs	$\Delta u_{max}$	$[\infty \infty]$
$\tau_u$	[8 8] hrs	$W_y$	$[1 1]$
$u_{min}$	[273.15 K 0 m <sup>3</sup> /h]	$W_{\Delta u}$	$[0 0]$
$u_{max}$	$[\infty \infty]$	$T_s$	1 hr

current MoD-based model has some limitations that can be addressed in future work. This includes research related to robustness to noisy databases, missing data, and high-dimensional data. Improved measures for the relevance of data points for local polynomial modeling beyond the current norm-based approach can also be considered.

#### 5. ACKNOWLEDGEMENT

Support for this research has been provided by NIH grants R01LM013107 and R01CA244777, and NSF grant CBET 2200161. The views presented in this paper are the authors' own and do not necessarily reflect the views of the NIH or the NSF.

#### REFERENCES

Bequette, B.W. (2003). *Process Control: Modeling, Design, and Simulation*. Prentice Hall Professional.

Braun, M.W. (2001). *Model-on-Demand Nonlinear Estimation and Model Predictive Control: Novel Methodologies for Process Control and Supply Chain Management*. Ph.D. thesis, Arizona State University, USA.

Carnerero, A.D., Ramirez, D.R., Limon, D., and Alamo, T. (2023). Kernel-Based State-Space Kriging for Predictive Control. *IEEE/CAA Journal of Automatica Sinica*, 10(5), 1263–1275.

Guillaume, P., Schoukens, J., Pintelon, R., and Kollar, I. (1991). Crest-factor minimization using nonlinear Chebyshev approximation methods. *IEEE Transactions on Instrumentation and Measurement*, 40(6), 982–989.

Häggblom, K. and Böling, J. (1998). Multimodel identification for control of an ill-conditioned distillation column. *Journal of Process Control*, 8(3), 209–218.

Khan, O., El Mistiri, M., Rivera, D.E., Martin, C.A., and Hekler, E. (2022). A Kalman filter-based Hybrid Model Predictive Control Algorithm for Mixed Logical Dynamical Systems: Application to Optimized Interventions for Physical Activity. In *2022 IEEE 61st Conference on Decision and Control (CDC)*, 2586–2593. IEEE.

Nandola, N.N. and Rivera, D.E. (2010). Model-on-Demand Predictive Control for Nonlinear Hybrid Systems With Application to Adaptive Behavioral Interventions. In *49th IEEE Conference on Decision and Control (CDC)*, 6113–6118. IEEE.

Nandola, N.N. and Rivera, D.E. (2013). An Improved Formulation of Hybrid Model Predictive Control with Application to Production-Inventory Systems. *IEEE Trans. Control Syst. Technol.*, 21(1), 121–135.

Piga, D., Formentin, S., and Bemporad, A. (2018). Direct Data-Driven Control of Constrained Systems. *IEEE Trans. Contr. Syst. Technol.*, 26(4), 1422–1429.

Rivera, D.E., Lee, H., Mittelmann, H.D., and Braun, M.W. (2007). High-purity distillation. *IEEE Control Systems Magazine*, 27(5), 72–89.

Stenman, A. (1999). *Model-on-Demand: Algorithms, Analysis and Applications*. Ph.D. thesis, Linköping University, Sweden.